Journal of Electroceramics (2018) 40:115–121
https://doi.org/10.1007/s10832-018-0110-9

Microstructures and dielectric properties of sol-gel prepared K-doped $CaCu_3Ti_4O_{12}$ ceramics

Zhenduo Wang[1] · Jianqin Guo[1] · Wentao Hao[1] · Ensi Cao[1] · Yongjia Zhang[1] · Li Sun[1,2] · Panpan Xu[3]

Received: 8 December 2016 / Accepted: 2 January 2018 / Published online: 19 January 2018

Abstract
K^+ doped $CaCu_3Ti_4O_{12}$ ceramics were prepared by the sol-gel method and sintered at different temperatures from 1040 °C to 1100 °C. The microstructures and various dielectric properties of $Ca_{1-x}K_xCu_3Ti_4O_{12-\delta}$ ceramics were investigated. Results of XRD indicate that the $Ca_{1-x}K_xCu_3Ti_4O_{12-\delta}$ samples exhibit a typical cubic structure. The grain size as well as the dielectric permittivity (ε') increase obviously with the increasing sintering temperature. The dielectric permittivity and dielectric loss (tanδ) measurements show strong frequency dependence in all the samples. A ε' value of about 2.3×10^4 and a low tanδ value of about 0.039 were observed at room temperature and 1 kHz in the $Ca_{0.99}K_{0.01}Cu_3Ti_4O_{12-\delta}$ (CKCTO) ceramics sintered at 1060 °C for 8 h, showing better dielectric properties than pure CCTO. Dielectric relaxations were observed in ε′/tanδ-T curves which may be related to the IBLC effect.

Keywords A.$CaCu_3Ti_4O_{12}$ · D.Dielectric properties · E.Sol-gel method

1 Introduction

In the past few years, miniaturization, lightening and multifunctionalization of the systems have been the key points in the electronic information technologies. Therefore, for dielectric materials, it is required to possess a higher dielectric constant, lower dielectric loss (tanδ) and better thermal stability. $CaCu_3Ti_4O_{12}$ (CCTO), with a cubic perovskite structure, has drawn considerable attention in the last decade. It shows an extremely high ε' value in a wide frequency range, which is practically independent of temperature between 100 K and 600 K [1–4]. Until now, the mechanism related to this material's electrical properties is not completely understood [5, 6]. However, it is now widely accepted that the high ε' is associated with the internal barrier layer capacitance (IBLC) effect [7–11]. It is also reported that dielectric properties depend on many extrinsic factors such as processing conditions and element doping [12–16].

In fact, besides the ε' of CCTO, the tanδ is found to be too high, limiting its practical applications [2]. Since the microstructure and dielectric properties of CCTO are strongly dependent on the doping elements and their concentrations, many groups have been trying to substitute the cations of CCTO using different elements, hoping to improve the dielectric properties. Some valuable results and methods have been reported continuously, such as Sm^{3+}, Mg^{2+}, Ni^{2+}, Zr^{4+}, Lu^{3+} and Y^{3+} doped CCTO [6, 12–16]. Besides, the sol-gel method is a common practice for preparing doped CCTO ceramics [17–19]. This method has several considerable advantages including accurate chemical stoichiometry, compositional homogeneity and lower crystallization temperature [20, 21].

Recently, our group have successfully synthesized pure CCTO [22], Zr^{4+} [23] and Mg^{2+} doped CCTO at the Ti^{4+} and Cu^{2+} site [14] by the sol-gel method. In previous work of other groups, proper Y^{3+} and Lu^{3+} doping at Ca^{2+} site was found to be able to improve the dielectric properties of CCTO [15, 16]. In this work,

✉ Li Sun
sunlitut@163.com

✉ Panpan Xu
359541889@qq.com

[1] College of Physics and Optoelectronics, Taiyuan University of Technology, Taiyuan 030024, People's Republic of China

[2] Key Lab of Advanced Transducers and Intelligent Control System, Ministry of Education, Taiyuan University of Technology, Taiyuan 030024, People's Republic of China

[3] College of materials science and engineering, Taiyuan University of Technology, Taiyuan 030024, People's Republic of China

stoichiometric $Ca_{1-x}K_xCu_3Ti_4O_{12-\delta}$ (x = 0, 0.01, 0.05, 0.1) ceramics were successfully prepared by the sol-gel method. The influences of K^+ doping and sintering conditions on the microstructures and dielectric properties were analyzed and discussed.

2 Experimental

$Ca_{1-x}K_xCu_3Ti_4O_{12-\delta}$ (CKCTO, x = 0, 0.01, 0.05, 0.1) powders were prepared by the sol-gel method. Appropriate amount of $Ca(NO_3)_2{\cdot}4H_2O$, KNO_3, $Cu(NO_3)_2{\cdot}3H_2O$, $[CH_3(CH_2)_3O]_4Ti$ and $C_6H_8O_7$ were dissolved in ethanol for a uniform mixing. The sol was obtained after magnetic stirring for about 30 min. Then the sol was stirred at 80 °C for about 5 h and dried at 100 °C for 16 h to form the gel. The precursor powders were obtained by sintering the gel at 650 °C for 2 h. The CKCTO precursor was then pressed into small pellets with a pressure of 350 MPa. The pellets were then sintered at different temperatures from 1040 °C to 1100 °C for 8 h. The structures of the prepared ceramic samples were investigated by X-ray diffraction with Cu-Kα radiation (MSAL-XD2 diffractometer). The fractured cross-sectional microstructures were investigated by a scanning electronic microscope (SEM, HITACHI S-520). The dielectric properties were investigated by a LCR meter (Agilent E4980A).

3 Results and discussion

The X-ray diffraction patterns of $Ca_{1-x}K_xCu_3Ti_4O_{12-\delta}$ ceramic samples sintered at 1060 °C for 8 h are shown in Fig. 1. The XRD peaks are well consistent with the values in the Committee for Powder Diffraction Standard card for CCTO (No. 75–2188). Lattice parameters are calculated to be 7.381 Å, 7.383 Å, 7.391 Å and 7.392 Å for x = 0, 0.01, 0.05, 0.1, respectively. The lattice parameter increases with the increasing K^+ doping concentration which may be due to the ion radius of K^+ (0.138 Å) is a little larger than Ca^{2+} (0.100 Å). Figure 2 shows the XRD patterns of $Ca_{0.99}K_{0.01}Cu_3Ti_4O_{12-\delta}$ ceramics sintered at 1040 °C, 1060 °C, 1080 °C and 1100 °C for 8 h. Similarly, these samples also show a cubic perovskite structure without a secondary phase, indicating K^+ has successfully substituted Ca^{2+} atom in CCTO. In addition, the x = 0.01 sample sintered at 1060 °C shows superior dielectric properties, which will be discussed later.

Figures 3 and 4 show the SEM images of the fractured surfaces for the CKCTO samples presented in Figs. 1 and 2, respectively. Histograms of the grain size

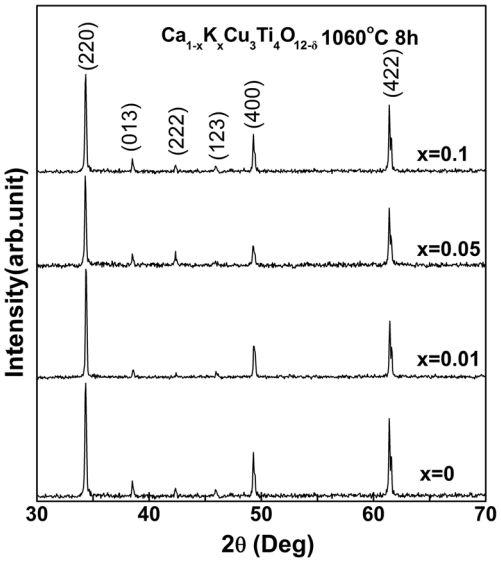

Fig. 1 The XRD patterns of $Ca_{1-x}K_xCu_3Ti_4O_{12-\delta}$ (x = 0,0.01, 0.05 and 0.1) ceramic samples sintered at 1060 for 8 h

distribution obtained from CKCTO samples are displayed in the corresponding insets. Obviously, all the samples are composed of the grain with sizes of several μm, and both K^+ doping concentration and sintering temperature (T_S) seems to show obvious impact on morphology. The average grain sizes estimated by a line-intercept technique from Fig. 3 for $Ca_{1-x}K_xCu_3Ti_4O_{12-\delta}$ ceramic samples sintered at 1060 °C are 3.38, 4.28, 5.65 and 8.21 μm, respectively, indicating K^+ doping is benefit for the growth of CCTO. Usually, the increasing of T_S also promotes the growth of grain size for ceramics. The average grain sizes for $Ca_{0.99}K_{0.01}Cu_3Ti_4O_{12-\delta}$ samples are 2.75, 4.28, 5.42,

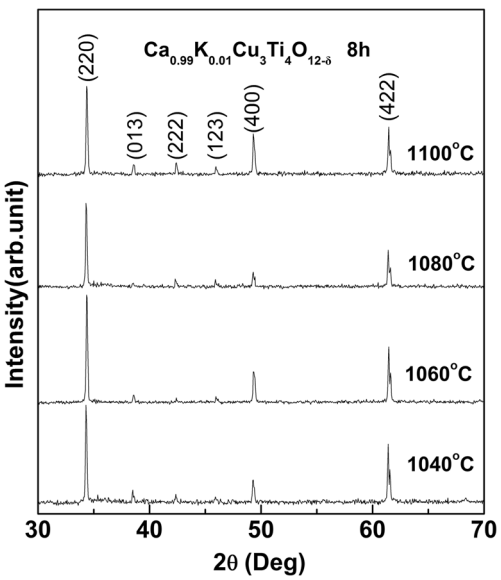

Fig. 2 The XRD patterns of $Ca_{0.99}K_{0.01}Cu_3Ti_4O_{12-\delta}$ ceramic samples sintered at 1040, 1060, 1080 and 1100 °C for 8 h

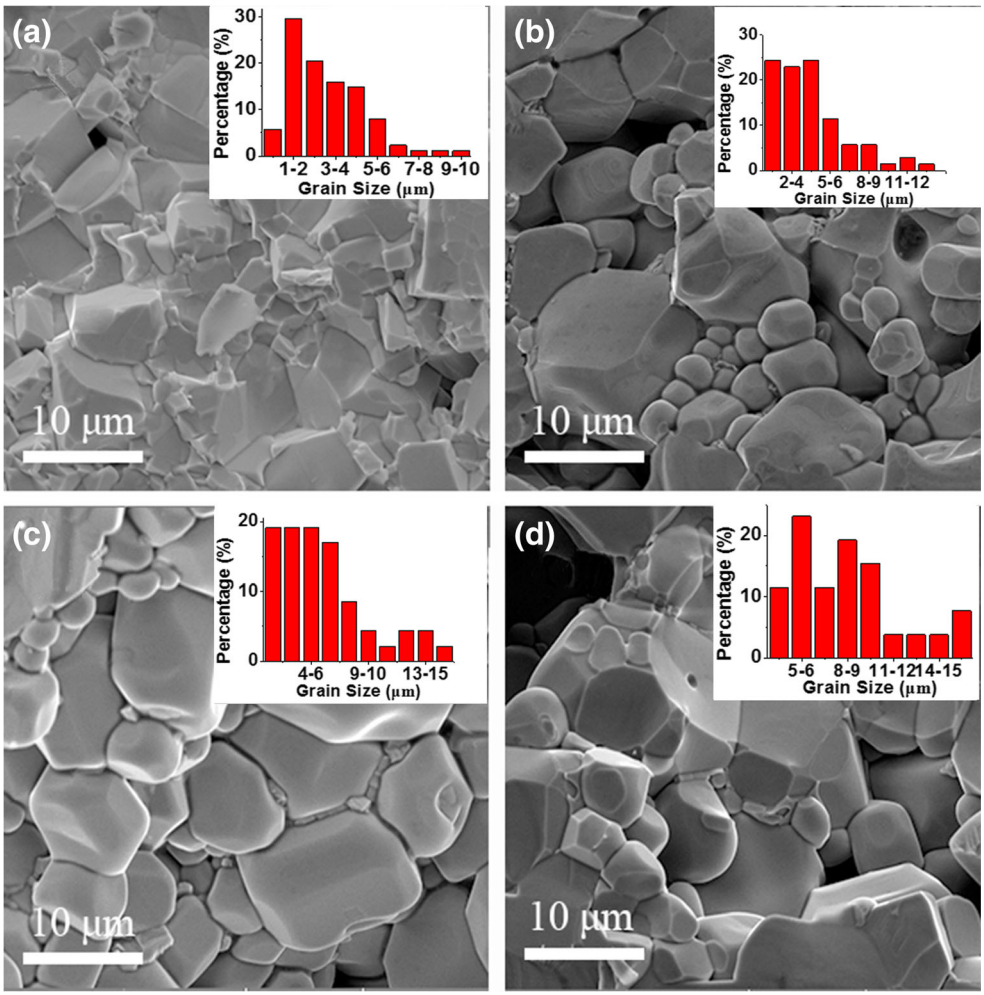

Fig. 3 The FE-SEM images of the fractured surfaces of $Ca_{1-x}K_xCu_3Ti_4O_{12-\delta}$ (x = 0,0.01, 0.05 and 0.1) ceramics sintered at 1060 for 8 h

8.51 μm, and the relative density (measured by the Archimedes' method) increases from 75.48% to 84.15% when T_S increases from 1040 °C to 1100 °C. In recent reports of pure CCTO, CuO_x-rich inter-granular phase, which commonly precipitates out of CCTO ceramics during sintering at higher temperatures, can be always detected by SEM [10, 11]. Schmidt et al. indicated that segregation of a Cu-rich phase out of CCTO ceramics was clearly detected when T_S is above 1050 °C. This secondary Cu-rich phase may exhibit high mobility, accumulate at the sample surfaces and may volatilize at about 1100 °C [10]. Töpfer et al. reported that sintering above 1050 °C leads to the formation of a bimodal grain size distribution, i.e., small and coarse grains form. And the coarse grains show a broad distribution of grain size when $T_S \geq 1050$ °C [11]. In this work, the secondary Cu-rich phase can be observed in Fig. 4(c) and (d) ($Ca_{0.99}K_{0.01}Cu_3Ti_4O_{12-\delta}$ samples sintered at 1080 °C and 1100 °C) but is not obvious in other CKCTO SEM images. Therefore, comparing with the results of pure CCTO discussed above, K^+ doping appears to inhibit the generation of Cu_xO phase. In addition, no diffraction peaks of Cu_xO are detected in Figs. 1 and 2, also indicating that the amount of CuO_x-rich inter-granular phase is rather small and below the detection limit of XRD.

Figure 5 shows the frequency dependence of ε' and tanδ for $Ca_{1-x}K_xCu_3Ti_4O_{12-\delta}$ ceramics sintered at 1060 °C for 8 h. All the K^+ doping concentration can increase the ε' value in entire measured frequency range, and the ε' values of the ceramic with x = 0.01 are significantly higher than other ceramics. However, ε' value then decreases with the increasing K^+ doping concentration. For dielectric loss, the sample with x = 0.01 shows a much lower value than other K^+ concentration samples when f < 70 kHz, and the tanδ value is about 0.039 at 1 kHz while the value is 0.09 for pure CCTO. As we know, the most important task for CCTO is to lower the large dielectric loss. Some groups have reported other cations doped at Ca^{2+} site, such as Y^{3+} and Lu^{3+}, etc. [15, 16]. In our work, a ε' value of $\sim 2.3 \times 10^4$ and a low tanδ value of ~0.039 were

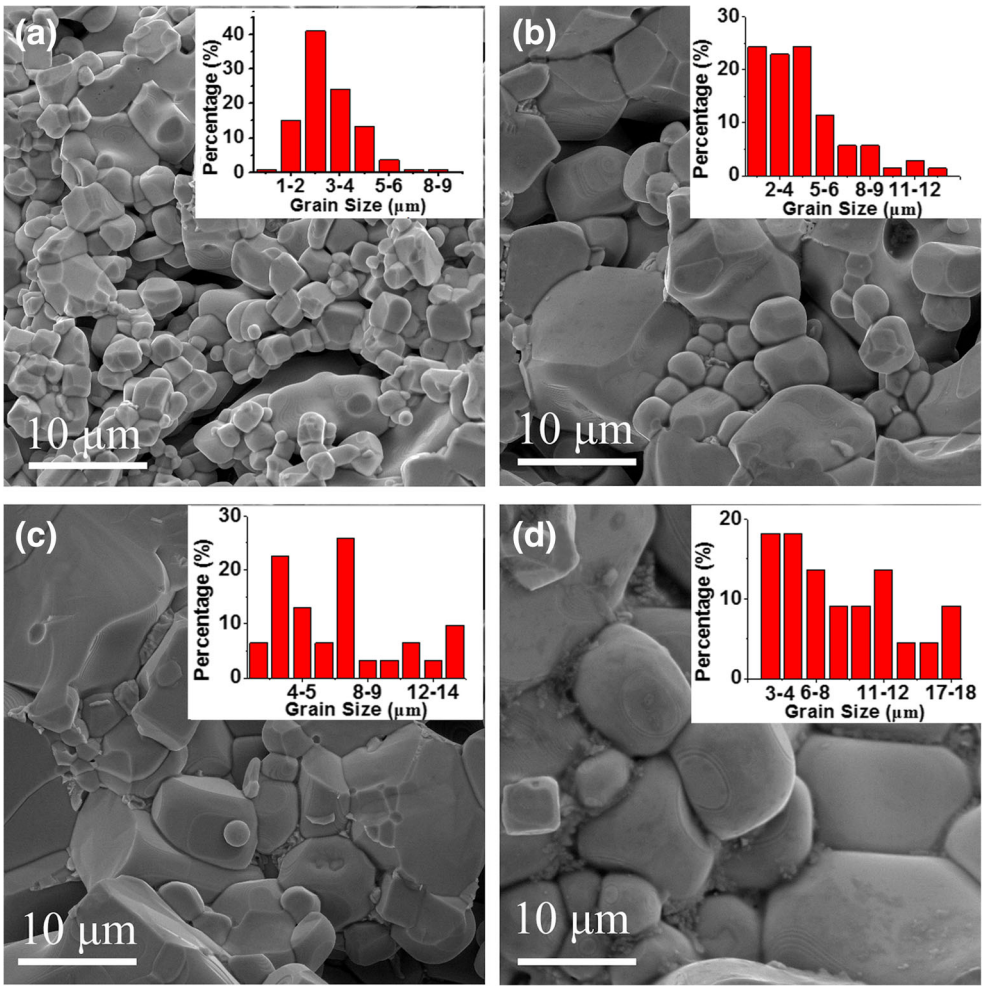

Fig. 4 The FE-SEM images of the fractured surfaces of $Ca_{0.99}K_{0.01}Cu_3Ti_4O_{12-\delta}$ ceramics sintered at 1040, 1060, 1080 and 1100 °C for 8 h

observed at RT and 1 kHz in the $Ca_{0.99}K_{0.01}Cu_3Ti_4O_{12-\delta}$ ceramics sintered at 1060 °C for 8 h. One can easily find that the ε' value is enough high, and the tanδ value (0.039) is much lower compared with the values of Y^{3+} and Lu^{3+} doping [15, 16]. The frequency dependence of ε' and tanδ for $Ca_{0.99}K_{0.01}Cu_3Ti_4O_{12-\delta}$ ceramics sintered at different T_S are shown in Fig. 6. The ε' values measured at 1 kHz and RT are 6477, 23,147, 27,329 and 35,530 for different $Ca_{0.99}K_{0.01}Cu_3Ti_4O_{12-\delta}$ ceramics. Recently, the one-step IBLC model is widely accepted as an effective method to study the dielectric properties of CCTO [3, 4, 7], and the ε′ of CCTO samples can be estimated by the equation below [7, 24].

$$\varepsilon_r \approx \varepsilon_{gb} \frac{A}{t} \tag{1}$$

ε_r and ε_{gb} in Eq. (1) represent the dielectric permittivity of the samples and grain boundary (GB), respectively. Meanwhile, A and t represent the average grain size of semiconducting grains and the average thickness of grain boundaries, respectively. The ε′ increases with the increasing average grain size as established by Eq. (1). The average grain size of $Ca_{0.99}K_{0.01}Cu_3Ti_4O_{12-\delta}$ ceramics increases obviously with the increasing sintering temperature. In other words, the ε' also increases with the increasing T_S (Fig. 6a). Similar correlation between T_S and dielectric permittivity has been detected previously in un-doped CCTO ceramics. Schmidt et al. indicated that increasing T_S promotes the formation of the IBLC structure. The differences in bulk and GB electric properties of CCTO ceramics are primarily driven by subtle chemical changes which is promoted by the heat treatment conditions [10]. Similarly, for CCKTO in this work, the higher the sintering temperature is, the larger the grain size grows, and the higher the ε' becomes. The trend is consistent with the Eq. (1) and un-doped CCTO ceramics [10]. The ε' plateau can be as high as about 3×10^4 for the CKCTO (x = 0.01) ceramic sample sintered at 1100 °C

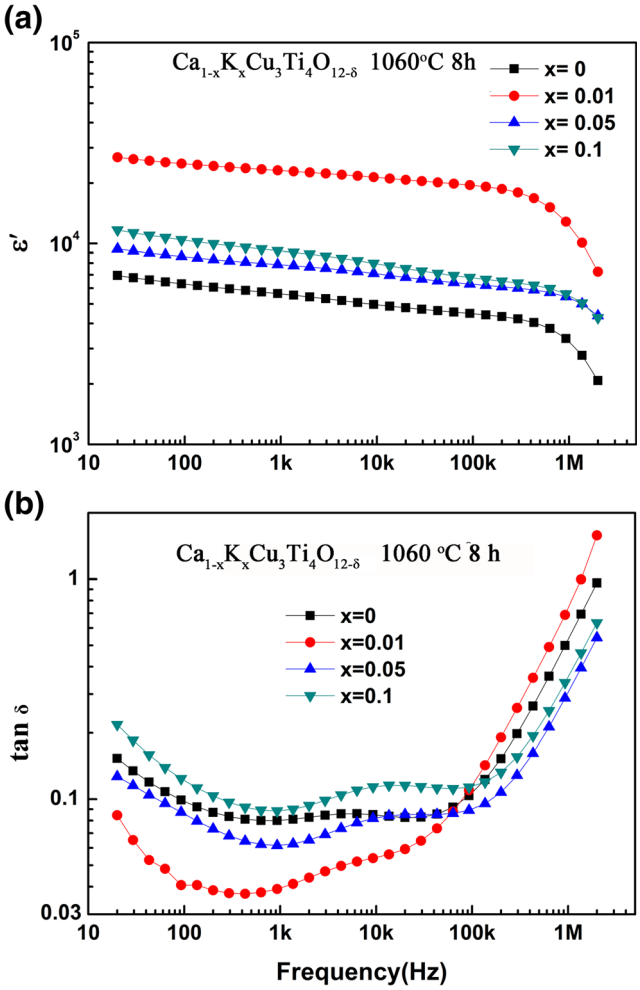

Fig. 5 The frequency dependence of ε′ (**a**) and tanδ (**b**) of $Ca_{1-x}K_xCu_3Ti_4O_{12-\delta}$ (x = 0, 0.01, 0.05 and 0.1) ceramic samples sintered at 1060 °C for 8 h

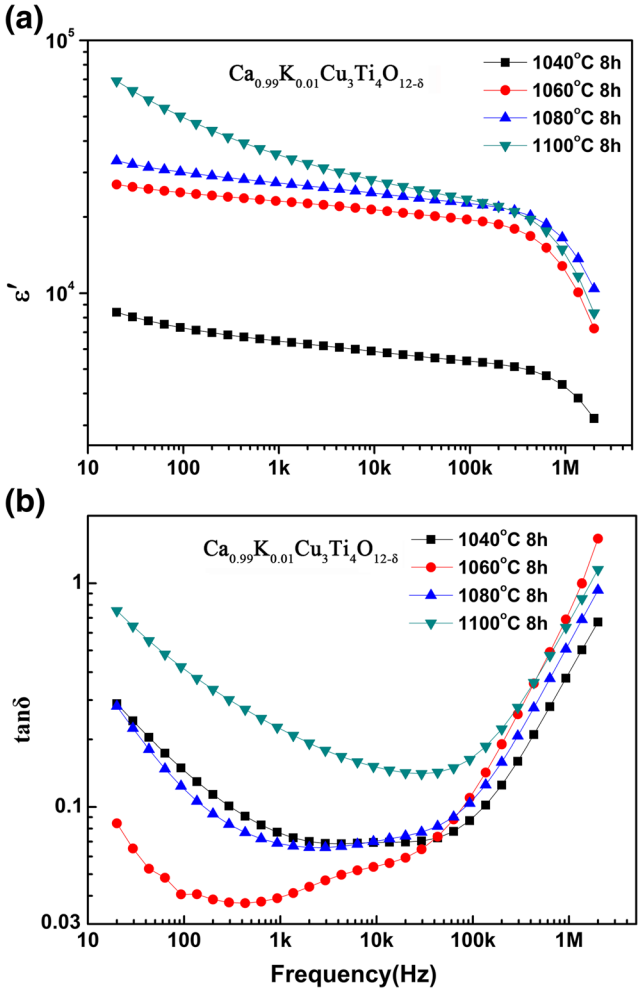

Fig. 6 The frequency dependence of ε′ (**a**) and tanδ (**b**) of $Ca_{0.99}K_{0.01}Cu_3Ti_4O_{12-\delta}$ ceramic samples sintered at 1040, 1060, 1080 and 1100 °C for 8 h

for 8 h. But at low frequency range (20 Hz - 40 kHz), the CKCTO ceramic sintered at 1060 °C showed the lowest tanδ value (Fig. 6b). Therefore, combining the dielectric results shown in Figs. 5 and 6, one can find that K^+ doping on Ca^{2+} site can improve both ε' and tanδ of CCTO only if the doping concentration and sintering condition was carefully selected.

On the other hand, the temperature/frequency stabilities of the ε'/tanδ are two important factors for practical applications. Fig. 7(a) and (b) show the temperature dependence of ε' and tanδ of the $Ca_{0.99}K_{0.01}Cu_3Ti_4O_{12-\delta}$ ceramic sintered at 1060 °C for 8 h measured at some typical frequencies. At low frequencies the increment in ε' with temperature is more pronounced than the high frequencies. For CCTO type ceramics, the dielectric permittivity can contain these contributions, the dipolar grain and the interfacial grain boundary and electrode contributions [9]. In dielectric materials, dipolar and interfacial polarizations play most important role at low frequencies. Both of these polarizations are strongly temperature dependent. The interfacial polarization increases with temperature due to the creation of crystal defects and dipolar polarization. The effect of temperature is more pronounced on the interfacial polarization than that of the dipolar polarization which results in the rapid increase in dielectric permittivity with increasing temperature at low frequencies [25, 26]. In the measured temperature range from 20 °C to 360 °C, one relaxation could be seen in the real part of the dielectric dispersion and a step change of ε' with temperature is observed in the ε'-T curve correspondingly (Fig. 7a). The characteristic temperature increases with the increasing frequency. The trend of tanδ is different from ε'. The tanδ value increases with the increasing frequency at RT, but decreases with the increasing frequency when the measured temperature reaches 360 °C. The temperature stability is higher for both ε' and tanδ at high frequency, since electronic and ionic polarizations are the main contributors and their temperature dependence is insignificant at high frequencies [23]. The dielectric

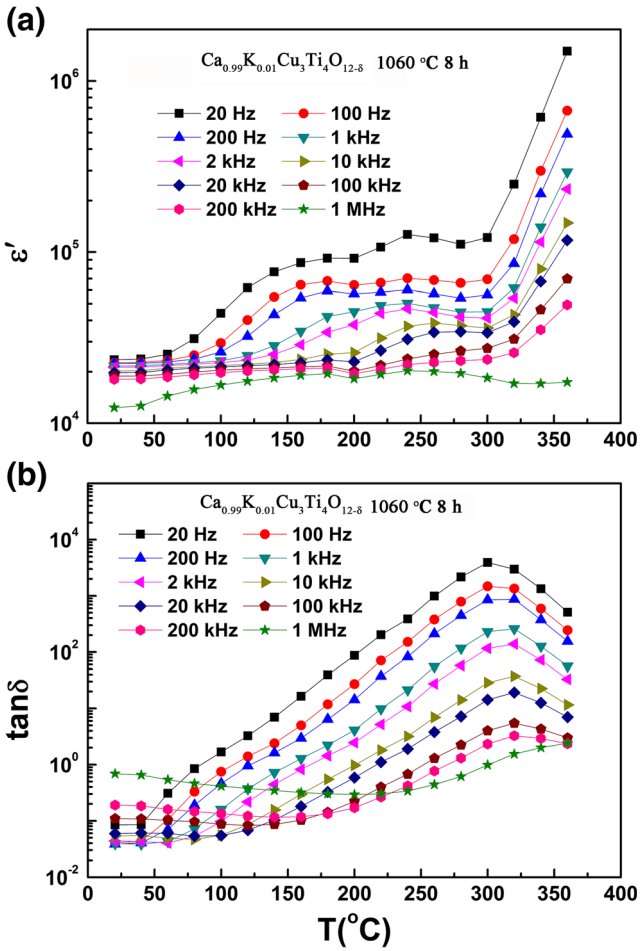

Fig. 7 The temperature dependence of ε′ (**a**) and tanδ (**b**) of $Ca_{0.99}K_{0.01}Cu_3Ti_4O_{12-\delta}$ ceramic sintered at 1060 °C for 8 h measured at some typical frequencies

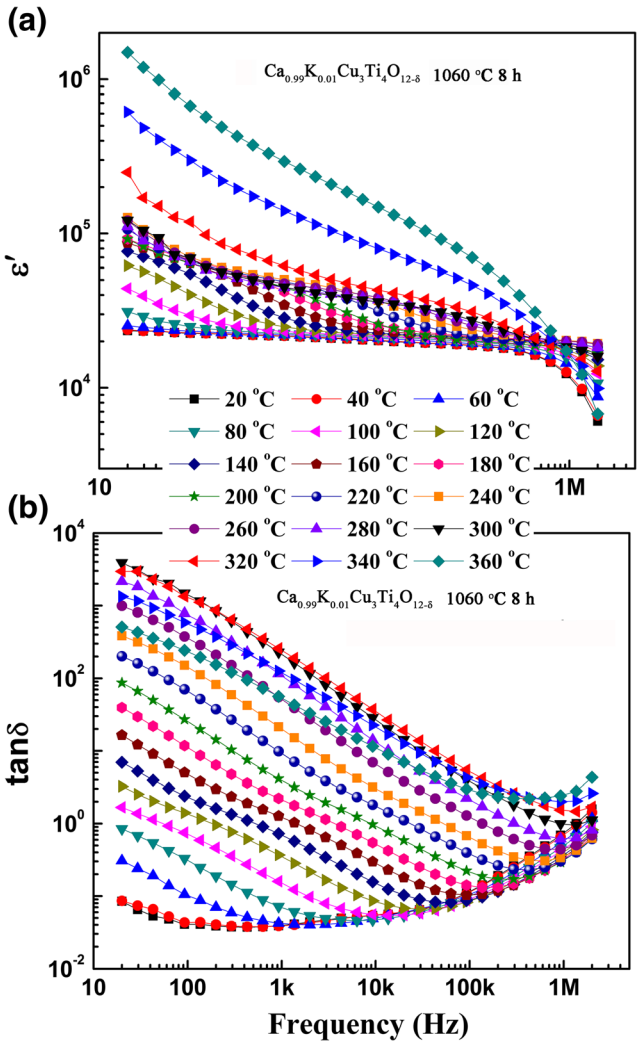

Fig. 8 The frequency dependence of ε′ (**a**) and tanδ (**b**) of $Ca_{0.99}K_{0.01}Cu_3Ti_4O_{12-\delta}$ ceramic sintered at 1060 °C for 8 h measured at some typical temperatures

behaviors of these ceramics resemble that found earlier in CCTO-like oxide ceramics [27]. Figure 8(a) and (b) show the frequency dependence of ε' and tanδ of the above $Ca_{0.99}K_{0.01}Cu_3Ti_4O_{12-\delta}$ ceramic. The ε' value increases with the increasing temperature below 700 kHz, and the frequency stability of ε' decreases accordingly. For temperatures below 80 °C, ε′ does not show significant dispersion until the frequency reaches 700 kHz, indicating there is only one Debye-like dielectric relaxation. As the temperature increases, ε′ at low frequency starts to increase notably. The characteristic frequency of dielectric dispersion clearly shifts to the higher frequencies with the increasing temperature (See Fig. 8a and b), and the frequency stability of tanδ decreases with the increasing temperature.

The complex impedance spectroscopies of the $Ca_{0.99}K_{0.01}Cu_3Ti_4O_{12-\delta}$ ceramic sintered at 1060 °C for 8 h measured at some typical temperatures are shown in Fig. 9. The inset in the upper right corner of Fig. 9 shows the temperature dependence of resistance of the GB for this ceramic. Usually, the resistance can be fitted with the formula [28]

$$R = R_0 exp(E_a/k_B T) \quad (2)$$

where R is the resistance, R_0 is a material constant, and E_a is the conductive activation energy. E_a is calculated to be 0.587 eV for the $Ca_{0.99}K_{0.01}Cu_3Ti_4O_{12-\delta}$ ceramic sintered at 1060 °C for 8 h. In addition, an equivalent circuit model has been proposed to clarify the dielectric properties of CCTO [29]. The equivalent circuit contains three RC elements (R_gC_g, $R_{gb}C_{gb}$, and R_xC_x, respectively) and a frequency dependent term Z_{UDR}, which represents the effect of hopping conduction of localized charge carriers [29]. And the contribution of R_xC_x may be identified as a non-ohmic electrode contact effect which has been established clearly by Ferrarelli

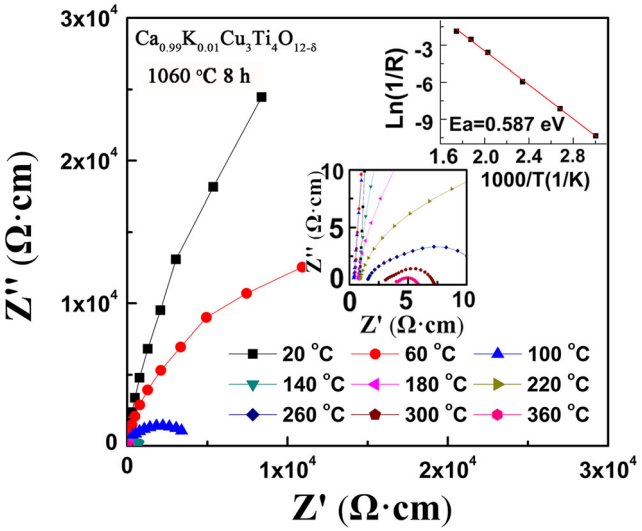

Fig. 9 The complex impedance spectroscopies of $Ca_{0.99}K_{0.01}Cu_3Ti_4O_{12-\delta}$ ceramic sintered at 1060 °C for 8 h measured at some typical temperatures. The inset shows the temperature dependence of resistance of the grain boundary

et al. [9]. From Fig. 9, one can find that the R_{gb} decreases with the increasing temperature. The non-zero intercept on Z' axis at high frequency data indicated the electrical response in the semiconducting part of the ceramic (inset of Fig. 9), which is the electrical response of the grains [13].

4 Conclusions

$Ca_{1-x}K_xCu_3Ti_4O_{12-\delta}$ ceramics were synthesized by the sol-gel method. XRD analysis indicates that the samples consist of a single phase. The grain size increases with the increasing sintering temperature and K^+ doping concentration. Both ε' and tanδ exhibit strong dependence on sintering condition and grain size. Giant ε' of ~2.3×10^4 as well as relatively low tanδ of ~0.039 can be observed in $Ca_{0.99}K_{0.02}Cu_3Ti_4O_{12}$ ceramics sintered at 1060 °C for 8 h measured at RT and 1 kHz. The tanδ can be lower than 0.05 in a relatively wide frequency range from 40 Hz to 6 kHz, which is desirable for practical applications. Proper sintering condition and K^+ doping concentration could strongly improve the IBLC structure and the dielectric property of CCTO.

Acknowledgements This work was supported by National Natural Science Foundation of China (No. 11404236, 11604234 and 51602214), Natural Science Foundation of Shanxi Province (No. 201601D202010 and 2015021026).

References

1. M.A. Subramanian, D. Li, N. Duan, B.A. Reisner, A.W. Sleight, J. Solid State Chem. **151**, 323 (2000)
2. A.P. Ramirez, M.A. Subramanian, M. Gardel, G. Blumberg, D. Li, T. Vogt, S.M. Shapiro, Solid State Commun. **115**, 217 (2000)
3. D.C. Sinclair, T.B. Adams, F.D. Morrison, A.R. West, Appl. Phys. Lett. **80**, 2153 (2002)
4. T.B. Adams, D.C. Sinclair, A.R. West, Phys. Rev. B **73**, 094124 (2006)
5. C.C. Homes, T. Vogt, S.M. Shapiro, S. Wakimoto, A.P. Ramirez, Science **293**, 673 (2001)
6. J. Boonlakhorn, P. Kidkhunthod, P. Thongbai, J. Eur. Ceram. Soc. **35**, 3521 (2015)
7. T.B. Adams, D.C. Sinclair, A.R. West, Adv. Mater. **14**, 1321 (2002)
8. J. Yang, M. Shen, L. Fang, Mater. Lett. **59**, 3990 (2005)
9. M.C. Ferrarelli, D.C. Sinclair, A.R. West, H.A. Dabkowska, A. Dabkowski, G.M. Luke, J. Mater. Chem. **19**, 5916 (2009)
10. R. Schmidt, M.C. Stennett, N.C. Hyatt, J. Pokorny, J. Prado-Gonjal, M. Li, D.C. Sinclair, J. Eur. Ceram. Soc. **32**, 3313 (2012)
11. R. Löhnert, R. Schmidt, J. Töpfer, J. Electroceram. **34**, 241 (2015)
12. T. Li, J. Chen, D. Liu, Z. Zhang, Z. Chen, Z. Li, X. Cao, B. Wang, Ceram. Int. **40**, 9061 (2014)
13. P. Thongbai, J. Jumpatam, B. Putasaeng, T. Yamwong, S. Maensiri, Mater. Res. Bull. **60**, 695 (2014)
14. L. Sun, R. Zhang, Z. Wang, E. Cao, Y. Zhang, L. Ju, J. Alloys Compd. **663**, 345 (2016)
15. J. Boonlakhorn, P. Kidkhunthod, B. Putasaeng, T. Yamwong, P. Thongbai, S. Maensiri, J. Mater. Sci. Mater. Electron **26**, 2329 (2015)
16. J. Boonlakhorn, P. Kidkhunthod, B. Putasaeng, T. Yamwong, P. Thongbai, S. Maensiri, Appl. Phys. A Mater. Sci. Process. **120**, 89 (2015)
17. S. De Almeida-Didry, C. Autret, C. Honstettre, A. Lucas, F. Pacreau, F. Gervais, Solid State Sci. **42**, 25 (2015)
18. D. Xu, C. Zhang, Y. Lin, L. Jiao, H. Yuan, G. Zhao, X. Cheng, J. Alloys Compd. **522**, 157 (2012)
19. X. Ouyang, M. Habib, P. Cao, S. Wei, Z. Huang, W. Zhang, W. Gao, Ceram. Int. **41**, 13447 (2015)
20. C.J. Brinker, G.W. Scherer, Sol-Gel Science, Academic Press (1990)
21. Y.G. Metlin, Y.D. Tretyakov, J. Mater. Chem. C **4**, 1659 (1994)
22. L. Sun, Z. Wang, Y. Shi, E. Cao, Y. Zhang, H. Peng, L. Ju, Ceram. Int. **41**, 13486 (2015)
23. L. Sun, Z. Wang, W. Hao, E. Cao, Y. Zhang, H. Peng, J. Alloys Compd. **651**, 283 (2015)
24. S. De Almeida-Didry, C. Autret, A. Lucas, C. Honstettre, F. Pacreau, F. Gervais, J. Eur. Ceram. Soc. **34**, 3649 (2014)
25. J. Sharma, N. Sharma, J. Parashar, V.K. Saxena, D. Bhatnagar, K.B. Sharma, J. Alloys Compd. **649**, 362 (2015)
26. V.L. Mathe, R.B. Kamble, Mater. Res. Bull. **48**, 1415 (2013)
27. W. Hao, J. Zhang, Y. Tan, W. Su, J. Am. Ceram. Soc. **92**, 2937 (2009)
28. Y. Song, X. Wang, X. Zhang, Y. Sui, Y. Zhang, Z. Liu, Z. Lv, Y. Wang, P. Xu, B. Song, J. Mater. Chem. C **4**, 6798 (2016)
29. W. Hao, J. Zhang, Y. Tan, M. Zhao, C. Wang, J. Am. Ceram. Soc. **94**, 1067 (2011)